PROTEINS: Structure, Function, and Genetics 25:12–27 (1996)

# RESEARCH ARTICLES

# Molecular Dynamics Study of Phospholipase $A_2$ on a Membrane Surface

**Feng Zhou and Klaus Schulten**

*Department of Biophysics, Physics and Beckman Institute, University of Illinois at Urbana-Champaign, Urbana, Illinois 61801*

*ABSTRACT* **The desolvation of lipid molecules in a complex of the enzyme human synovial phospholipase $A_2$ with a lipid membrane is investigated as a mechanism that enhances the overall activity of the enzyme. For this purpose the interaction of the enzyme phospholipase $A_2$ with a dilauryl-phosphatityl-ethanolamin (DLPE) membrane monolayer surface has been studied by means of molecular dynamics simulations. Two enzyme-membrane complexes, a loose and a tight complex, are considered. For comparison, simulations are also carried out for the enzyme in aqueous solution. The conformation, dynamics, and energetics of the three systems are compared, and the interactions between the protein and lipid molecules are analyzed. Free energies of solvation are calculated for the lipid molecules in the enzyme–membrane interface. Along with the calculated dielectric susceptibility at this interface, the results show the desolvation of lipids in a tightly bound, but not in a loosely bound protein-membrane complex. The desolvated lipids are found to interact mainly with hydrophobic protein residues, including Leu-2, Val-3, Ala-18, Leu-19, Phe-24, Val-31, and Phe-70. The results also explain why the turnover rate of phospholipase $A_2$ complexed to a membrane is enhanced after a critical amount of negatively charged reaction product is accumulated.**



**Key words: protein-membrane interaction, free energy perturbation, lipid desolvation**

## INTRODUCTION

Phospholipase $A_2$ ($PLA_2$) complexes with membrane surfaces in a scooting mode and catalyzes the hydrolysis reaction of the *sn*-2 ester bond of phospholipids.[1–3] The enzyme plays an important physiological role; one of the reaction products, arachidonic acid, is an important metabolic intermediate for producing eicosanoids, which are regulatory factors implicated in a wide range of physiological and pathological states.[4] There exist at least two types of $PLA_2$, the 14 kd extracellular type[5] and the 80 kd intracellular type.[6] The extracellular type has been more thoroughly investigated due to its availability and structural simplicity. This type occurs in a variety of snake venoms and mammalian exocrine glands. Detailed reviews are available for the extracellular $PLA_2$ enzyme.[1,2,7–9]

The structure of extracellular $PLA_2$ has been solved for many species.[8,10–14] These structures show a high degree of similarity (e.g., the residues in the enzyme active site are essentially unchanged among the structures solved) and support the previously proposed mechanism of the enzyme reaction[10] involving a catalytic triad formed by a catalytic water, a histidine, and an aspartic acid at a site removed from the enzyme surface. The high degree of similarity in the three-dimensional structure between different species and the large number of disulfide bonds (seven for human synovial $PLA_2$) suggest that the enzyme structure is highly robust.

The structure of $PLA_2$ also revealed that the residues identified as interacting with the membrane form a flat surface. In the case of porcine pancreatic $PLA_2$, for example, residues Ala-1, Arg-6, Met-20, Trp-3, Trp-31, Tyr-19, and Tyr-69, which have been implicated in the binding of $PLA_2$ to membrane surfaces[1], are located on one of the flat surfaces of $PLA_2$, the so-called interfacial recognition site.[5,15]

$PLA_2$ displays a much higher activity on lipid aggregates, such as micelles or lipid bilayers, compared with the enzyme acting on lipid monomers in aqueous solution.[5,15,16] One must note in this re-

Received June 29, 1995; revision accepted January 16, 1996.

Address reprint requests to Klaus Schulten, Beckman Institute, University of Illinois at Urbana-Champaign, Urbana, IL 61801.

spect that the interfacial catalysis of $PLA_2$ involves a series of reaction steps (such as complex formation, scooting, lipid extraction from the membrane, and the actual reaction step) that require a specific kinetic analysis beyond conventional schemes.[16] The present study focuses solely on the enhancement of the overall enzyme reaction through effects that favor binding of lipids to the active side. Related to this reaction step is the observation that the activity of $PLA_2$ varies by two orders of magnitude on membrane surfaces depending on the physicochemical properties of the membrane-water interface, such as the membrane surface charge density,[17,18] membrane defects,[19] and membrane phase properties.[20,21]

The origin of the enhancement of catalytic activity is not clearly understood. One class of models attributes the enhanced activity to changes in the $PLA_2$ enzyme molecule upon complexing to membranes or micelles, e.g., to a conformational change of the enzyme or a dimerization of the enzyme on the membrane surface.[22–24] A second class of models explains the enzyme activity through changes in the substrate, the phospholipid molecule: the head group of the lipids in membranes or micelles becomes desolvated through $PLA_2$ even before entering the enzyme active site, i.e., $PLA_2$ destabilizes the lipids energetically at the membrane/micellar surface and thereby decreases the free energy barrier of binding to the active site. In fact, fluorescence and nuclear magnetic resonance (NMR) experiments on porcine pancreatic $PLA_2$ suggest that Trp-3 is in a more hydrophobic environment when the protein is bound on membrane surfaces,[25–28] e.g., the absence of an isotope effect on the fluorescence quantum yield, when $D_2O$ solution is used, suggests that Trp-3 is shielded from bulk aqueous solution. Experiments also suggest that the ligated $Eu^{3+}$ ion (used in place of the calcium ions normally bound to $PLA_2$) is coordinated by fewer water molecules in the protein-membrane complex compared with ligation for the protein in aqueous solution.[29] These observations suggest that the membrane surface is desolvated in the protein-membrane complex. The findings reported below corroborate this explanation.

The proenzyme of mammalian pancreatic $PLA_2$, which has five to eight extra residues at the N-terminus, reacts with lipid substrates in aqueous solution like the normal enzyme, but does not exhibit the activity enhancement on membrane surfaces observed for $PLA_2$.[5,15] It is known that pro-$PLA_2$ does not show tight binding to the membrane surface. In the proenzyme–membrane system, the fluorescence spectrum of Trp-3 does not change appreciably compared with aqueous solution; also an isotope effect due to $D_2O$ is observed.[26] In some species, the proenzyme complexes to membrane surfaces with different characteristics compared with those of $PLA_2$. Studies[30] of $PLA_2$s treated by monoalogue, which modified the protein lysine residues including Lys-6 in the interfacial recognition site, indicate a behavior similar to that of the proenzyme. The modified enzyme does bind to negatively charged dimyristic-phosphatidyl-methanol (DMPM) vesicles, but does not show a desolvation effect of Trp-3 and does not exhibit interfacial activation even though the activity toward monomeric lipid substrate is largely preserved. One can conclude that $PLA_2$ can bind to the membrane in two modes, a loose, nonactivated mode as well as a tight, fully functional mode, and that dehydration of the membrane surface occurs only for the latter.

$PLA_2$ is known to associate much more favorably with negatively charged membrane surfaces compared with zwitterionic membrane surfaces. The association constants of $PLA_2$s from various sources are about $10^{10}$ times larger on DMPM lipids compared with dimyristic-phosphatidyl-choline (DMPC) lipids,[31] and the enzyme digests a whole vesicle of the former lipids in scooting mode. Even for vesicles of zwitterionic lipids, $PLA_2$ displays much tighter binding when the negatively charged reaction product fatty acid or any other negatively charged fatty acid accumulate beyond a critical concentration and the reaction becomes much faster.

One of the extracellular $PLA_2$s that are known to interact specifically with negatively charged membranes is human synovial $PLA_2$.[32–35] Compared with $PLA_2$s from other species, human synovial $PLA_2$ is highly positively charged. Its role in human inflammatory diseases has motivated studies of the interaction between the enzyme and membranes with the aim of designing inhibitors.[36] Due to its importance, human synovial $PLA_2$ has been chosen as the subject of our study.

The interfacial recognition site (IRS) of human synovial $PLA_2$ is shown in Figure 1. A cluster of hydrophobic residues (Leu-2, Val-3, Ala-18, Leu-19, Phe-24, Val-31, and Phe-70) is found in the central part of the IRS, forming the entrance to a narrow hydrophobic binding pocket. The majority of the remaining residues of the IRS are polar, neutral residues. Positively charged residues (Arg-34, Lys-53, Lys-57, Lys-69, Arg-58, Arg-92, Lys-123, His-124, Arg-126, and Arg-131) as well as negatively charged residues (Glu-16, Glu-56, and Asp-89) are found on the edges of the IRS region.

## MATERIALS AND METHODS

To study desolvation of lipid head groups and the effect of negatively charged lipids in a $PLA_2$–membrane complex, molecular dynamics simulation and free energy perturbation calculations are applied to free and membrane-complexed human synovial phospholipase $A_2$,[13,14] representing the membrane by a monolayer consisting of 100 DLPE lipids.

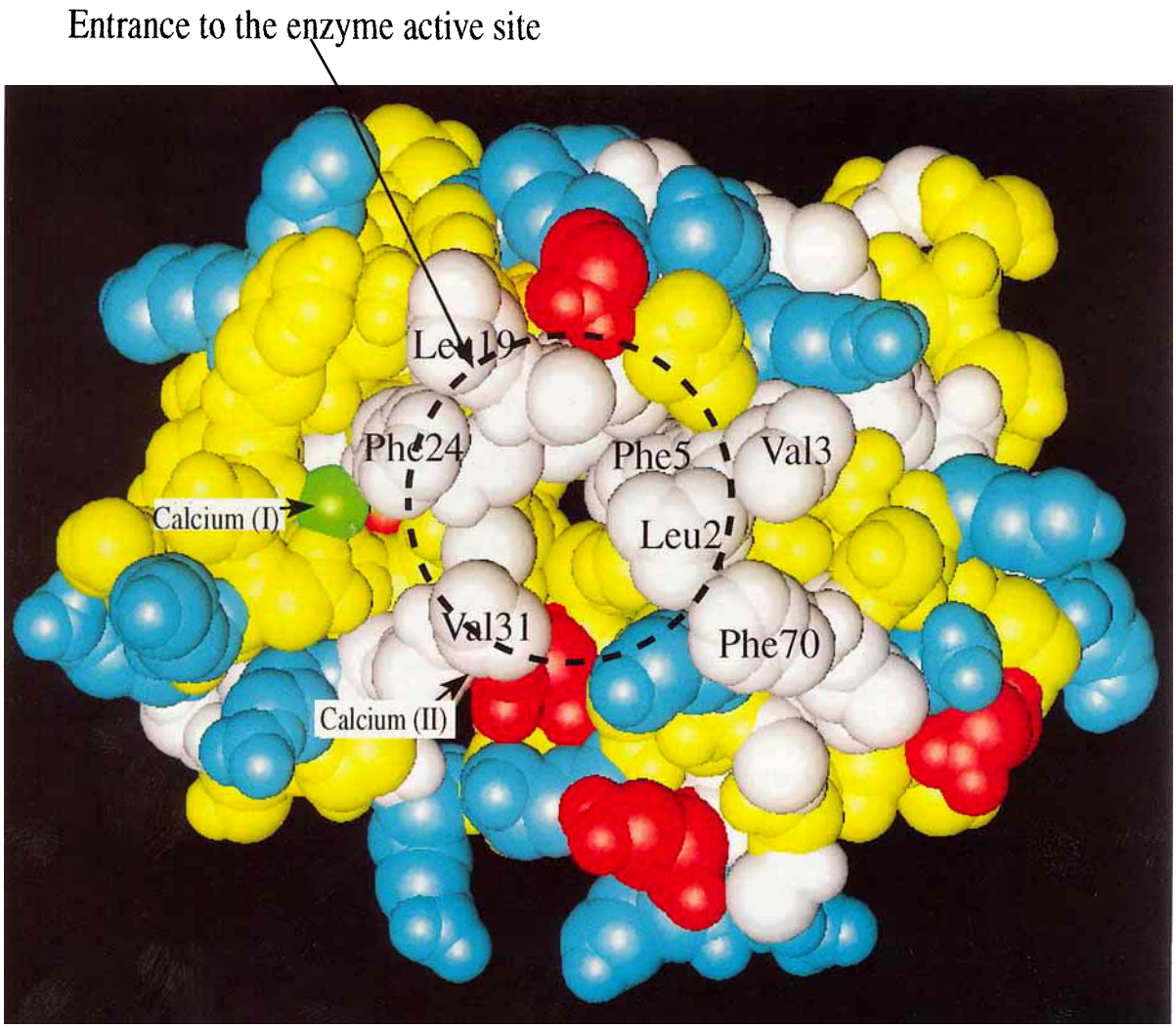


Fig. 1. Interfacial recognition site of $PLA_2$. Residues on the protein surface are colored according to their physicochemical properties. Hydrophobic residues are colored in white; neutral, but polar, residues in yellow; positively charged residues in blue; negatively charged residues in red.

**Construction of Models of $PLA_2$–Membrane Complexes**

The structure of human synovial $PLA_2$, reported in Scott et al.,[14] contained only one calcium ion, calcium I, ligated in the active site of the protein; this calcium ion is experimentally known to associate strongly with the protein and is absolutely required for the enzyme activity.[34] An additional calcium ion, calcium II, was found in the structure for the $PLA_2$–inhibitor complex.[14] However, the $PLA_2$ structure solved in Wery et al.[13] did not contain calcium ions. It is not clear whether the second calcium ion should be present in the $PLA_2$–membrane complexes, even though the first calcium is clearly necessary for the enzyme to be functional on the membrane surface. In this study, we have assumed that a second calcium ion plays a functional role in the enzymatic reaction, as suggested in Scott et al.[8] and hence we added it to the protein. Accordingly, we chose as an initial structure that reported in Scott et al.[14] (1POE in the Brookhaven Protein Data Bank), which contains two calcium ions and actually also an inhibitor, which, however, was subsequently deleted. Furthermore, for the initial structure we employed a monolayer of the equilibrated DLPE membrane bilayer in excess water as prepared in Zhou and Schulten.[37] The direction of the membrane normal was chosen as the z-axis. We restricted the simulations to a monolayer, instead of a bilayer, to reduce the computational effort significantly. The restriction is justified on the ground that many $PLA_2$s actually function on a membrane monolayer.[22,38] Based on the surface area of the $PLA_2$ IRS, one expects about 40 lipid molecules to be in

contact with the enzyme in a $PLA_2$–membrane complex.[9] The membrane monolayer employed in the present study consisted of 101 DLPE lipid molecules, a number large enough to avoid strong boundary effects.

The protein surface brought into contact with the DLPE monolayer was chosen according to the suggestion in Slotboom et al.[1] The resulting enzyme–membrane complexes are shown in Figure 2. The relative orientation of the protein with respect to the membrane was adjusted by rotation around the $x$- and the $y$-axes, such that the experimentally identified[1] IRS assumed an optimal contact with the lipid head groups. For this purpose, we employed the molecular graphics program VMD.[39,40]

The depth of the penetration of the enzyme into the membrane monolayer is not precisely known from experimental data. As discussed in the introduction, experimental evidence[1] suggests that $PLA_2$s associate with membrane surfaces in possibly two different forms, and surface activation arises only in a tightly associated form, e.g., for membranes with negatively charged lipids.[9] In the present study, two $PLA_2$–membrane complexes were constructed, differing in the protein-membrane distance by about 2.5 Å, corresponding to a tightly (complex$^T$) and a loosely (complex$^L$) bound protein–membrane complex. The protein residues in contact with the membrane surface are shown explicitly in Figure 2; their identities and position are indicated in bold letters in the amino acid sequence of the enzyme:

NLVNF**HR**MIKLTTGKE**AAL**S**Y**GF
YGCHCGVGGRGSPKDATDRCCVTHDCC[50]
YKRLEKRGCGTKFLSY**KF**SNSGSRI
TCAKQDSCRSQLCECDKAAATCFAR[100]
NKTTYNKKYQ**YY**SN**K**HCRGSTPRC.

The relative positions of the protein and membrane for the two complexes are compared in Figure 2. In case of complex$^L$, the protein does not penetrate into the membrane head group region, the protein and the membrane being separated by a thin layer of water molecules. Such conformation corresponds to a state in which the protein associates with the membrane attracted through electrostatic forces, but does not form close molecular contacts, leaving membrane head groups unperturbed. In the case of complex$^T$, in contrast, the side chains of the protein residues in the IRS penetrate into the phosphotidylethanolamine head groups, and a few bulky residues penetrate as far as the glycerol backbone region.

The water molecules surrounding $PLA_2$ and membrane were taken from the previously simulated DLPE membrane bilayer–water interface reported in Zhou and Schulten,[37] in which the water molecules solvating the lipid head groups were already equilibrated. To ensure complete solvation of the protein and to fill a hemispherical region with a radius of 43 Å, further water molecules, from a previously equilibrated periodic box of water provided by the program XPLOR,[41] were added to the system. The origin of the hemisphere was placed at the origin of the coordinate system, located at the protein–membrane interface. Water molecules with oxygen atoms closer than 1.6 Å to any protein or lipid atom were deleted, using a procedure similar to that employed in Zhou and Schulten.[37] The chosen size of the water hemisphere is large enough to solvate all protein atoms and lipid molecules in the central region of the membrane monolayer. Complex$^T$ and complex$^L$ contained altogether 16,339 and 15,583 atoms, respectively.

Another model, complex$^A$ (aqueous), in which $PLA_2$ is solvated only by water molecules, was constructed for a comparison with complex$^L$ and complex$^T$. The structure of $PLA_2$ used was the same in the latter complexes. Water molecules were added to fill in a cylindrical region defined by $\sqrt{x^2+y^2} < 32\text{Å} - 21.5\text{ Å} < z < 21.5\text{ Å}$ using procedures similar to the ones employed for complex$^L$ and complex$^T$. All protein atoms were solvated by at least an 8 Å thick water layer. The resulting system contained 3,790 waters and, altogether, 12,601 atoms.

### Parameters and Simulation Protocols

The CHARMm[42] united atom force field was used for protein, lipid, and water molecules. The parameters of the DLPE lipid molecules were described previously.[37] The molecular dynamics simulations were carried out using the program PMD.[43] Long-range Coulomb forces were calculated using the fast multipole algorithm in combination with a multiple timestep algorithm.[37]

Repulsive harmonic potentials were applied to water oxygen atoms and lipid atoms to provide a nonrigid boundary for the system. In simulations for complex$^L$ and complex$^T$, the boundary for water molecules was defined as a hemisphere $\sqrt{x^2 + y^2 + z^2} < 45$ Å, $z > -15.0$ Å. The radius of the sphere was chosen 2 Å larger than the radius used to place water molecules when the complexes were constructed. For lipid molecules, the boundary was defined as that of a cylinder $\sqrt{x^2 + y^2} < 43$ Å, following Zhou and Schulten.[37] In simulations for complex$^A$, the system boundary was defined as that of a cylinder with $\sqrt{x^2 + y^2} < 34$ Å, $-23.5\text{ Å} < z < 23.5$ Å. A harmonic potential with a force constant of 0.1 kcal/mol Å$^2$ was applied for all atoms diffusing out of the boundaries.

Molecular dynamics simulations, carried out for complex$^T$, complex$^L$, and complex$^A$ after 200 steps of energy minimization, will be referred to as simulation$^T$, simulation$^L$, and simulation$^A$, respectively. The procedures used to heat, equilibrate, and sam-

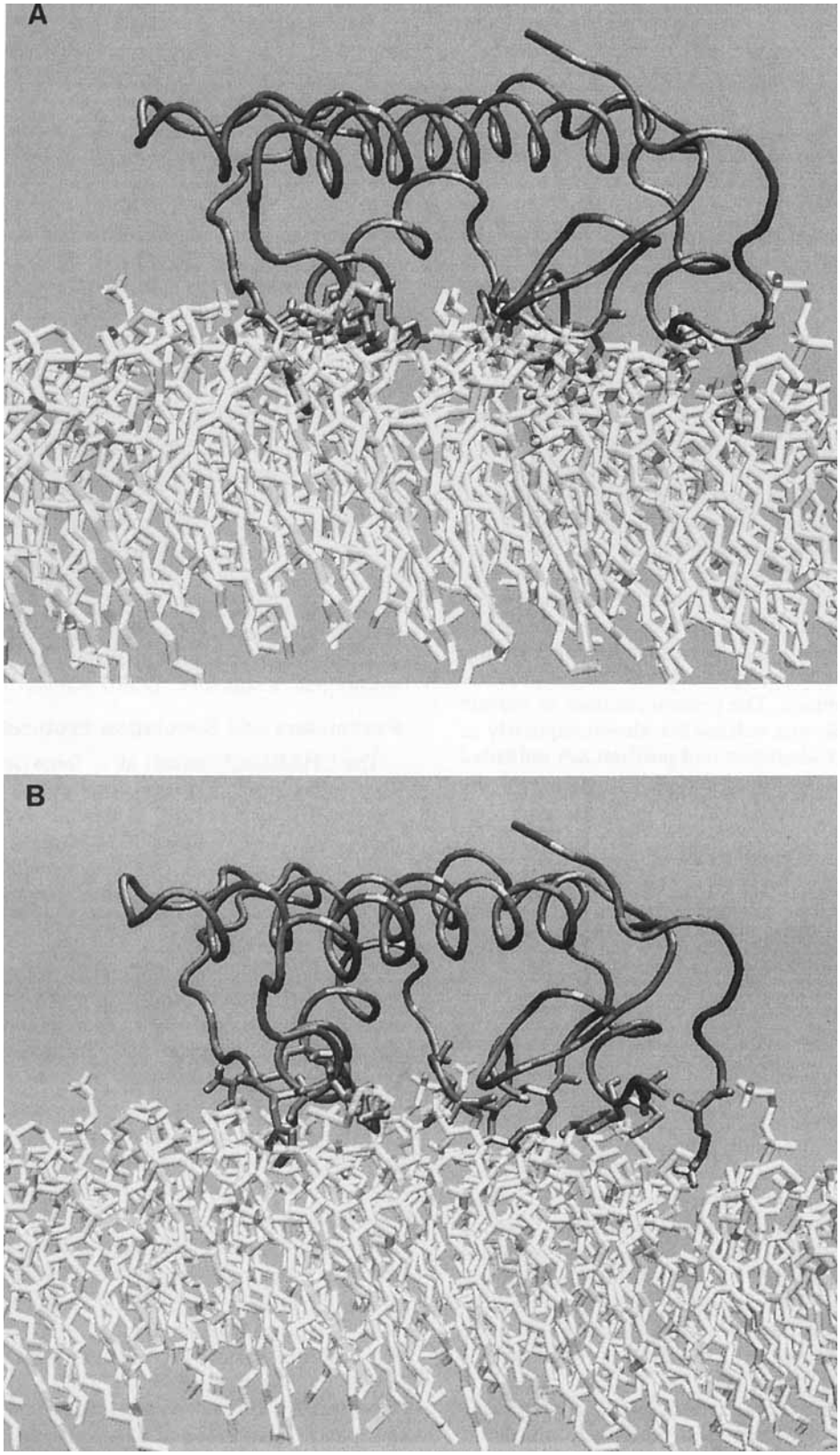


Fig. 2. Views of the relative position of the protein and membrane surface in complex$^T$ (**A**) and complex$^L$ (**B**). The protein backbone (top) and lipid molecules (bottom) are shown. The protein residues at the protein-membrane interface are shown explicitly and are in the middle.

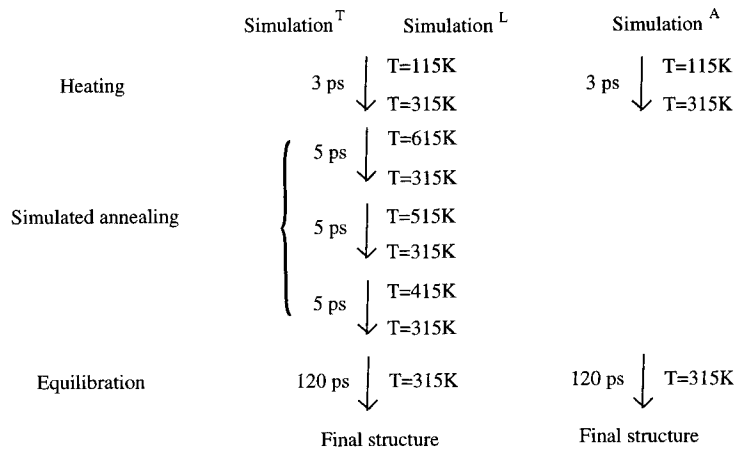


Fig. 3. Procedures adopted for simulations complex$^L$, complex$^T$, and complex$^A$ (see text). Initial heating started at 115 K and proceeded to 315 K within 3 ps. Simulated annealing was carried out for complex$^L$ and complex$^T$ for 15 ps each. Equilibration for all three complexes was carried out subsequently for 120 ps at 315 K, a temperature at which the DLPE membrane is in the liquid crystal phase.

ple the systems are summarized in Figure 3. The trajectories of the last 40 ps of simulation$^T$, simulation$^L$, and simulation$^A$ were recorded every 50 fs and were used for data analysis.

### Free Energy Calculation

In case of complex$^T$, to study the effect of PLA$_2$ on the solvation energy of membrane lipids, free energy calculations were performed using the perturbation method.[44,45]

To study the possible effect of deprotonation of the ethanolamine head group on the lipid-protein interaction, a number of simulations (simulation$^T_{negative}$) were carried out in which the charges of the groups $-CH_2NH_3^+$ of all lipid molecules were reduced. The net charge of this group was reduced from 1.0 to 0.95, 0.88, 0.80, and 0.70 by uniformly rescaling charges on all atoms in the group, respectively, in four separate simulations. As a result, each lipid head group had a net charge of −0.05, −0.12, −0.20, and −0.30 in the resulting systems. The starting structure of the simulations was the final configuration obtained through simulation$^T$ (after 120 ps molecular dynamics at 315 K). The change in free energy, when the charge of a lipid $-CH_2NH_3^+$ group is changed from $q_1$ to $q_2$, was evaluated by means of the expression

$$\delta G_{q_1,q_2} = k_B T \ln\left\langle \exp\left[ E_+ \frac{q_2 - q_1}{2.0} \Big/ (q_2 k_B T) \right] \right\rangle_2 - k_B T \ln\left\langle \exp\left[ -E_+ \frac{q_2 - q_1}{2.0} \Big/ (q_1 k_B T) \right] \right\rangle_1 \quad (1)$$

Here $E_+$ is the electrostatic potential energy of the $-CH_2NH_3^+$ head group. The subscripts 1 and 2 refer to the simulation on which the ensemble average is based: in case of $\langle \cdots \rangle_j$ a molecular dynamics trajectory for a $-CH_2NH_3^+$ head group charge of $q_j, j = 1,2$ is employed. The first term on the r.h.s. of Equation 1 corresponds to the free energy change when the charge of the lipid $-CH_2NH_3^+$ group is altered from $\frac{1}{2}(q_1 + q_2)$ to $q_2$; the second term corresponds to the free energy change for a charge change $q_1 \rightarrow \frac{1}{2}(q_1 + q_2)$.

To study the effect of PLA$_2$ on lipid head group solvation, a similar set of four simulations (simulation$^T_{reduced}$) was carried out. In this set the atomic charges of both the positive $-CH_2NH_3^+$ and the negative $-CH_2PO_4^-CH_2$ groups were uniformly scaled by the same factor, the net charge of each lipid remaining zero. The scaling factors were 0.95, 0.88, 0.80, and 0.70, i.e., the same as in simulation$^T_{negative}$. For each simulation of the type simulation$^T_{negative}$ and simulation$^T_{reduced}$, 30 ps equilibration and 10 ps data collection dynamics were performed. A total of 350 energy data points were sampled to determine the free energy changes. Using only a subset of the data (200 data points) gave results very similar to those using the entire data set, showing that enough data points were employed and that the free energy values had converged. The free energy difference between different lipid head groups charge states corresponding to scaling factors 1.0 and 0.64 were calculated by adding the energy differences for pairs of intermediate scaling factors.[7]

## RESULTS

In this section we characterize the properties of the enzyme–membrane complexes, focusing in particular on physicochemical properties related to the solvation of lipid head groups and relevant for the binding of lipids to PLA$_2$.

## Electron Density and Susceptibility Profile

The electron density of the protein, membrane, and water molecules at 120 ps of simulation$^T$ and simulation$^L$ are shown in Figure 4. The electron densities are calculated for all atoms within a cylinder of 15 Å radius normal to the $x,y$-plane. Comparison with the electron density of the complexes at the beginning and at the end of the simulations reveals that the relative positions of protein and membrane remain essentially unaltered. Changes, however, are recognized for water molecules in the protein–membrane interface; the corresponding electron density did not change appreciably during the course of simulation$^T$, but increased during simulation$^L$, indicating that water molecules are diffusing into the protein–membrane interface and solvating the lipid head groups. The changes developed, however, mainly during the first 80 ps of simulation$^L$, and densities remained essentially constant afterwards. In complex$^T$, less water is found in the protein–membrane interface compared with complex$^L$. At 120 ps, the density of water molecules in the protein–membrane interface was estimated through calculation of the integral water density (integrating water density up to a $z$-value $d$ where $d$ is a variable parameter) to be 30% and 65% of the bulk water density for complex$^T$ and complex$^L$, respectively.

The dielectric susceptibility determined for the membrane-protein interface is presented in Figure 5. The susceptibilities were calculated from fluctuations of the electrostatic polarization along the $z$-axis as described in Zhou and Schulten[37] using the trajectories from 100 ps to 120 ps of simulation$^T$ and simulation$^L$. To study the influence of the protein on the dielectric susceptibility, two calculations were carried out in which the radius of the sampling cylinders differ. In one calculation, the susceptibility due to atoms within a radius of 10 Å in the $x,y$-plane was evaluated; in this area the protein surface consists mainly of hydrophobic residues. In another calculation, a larger radius of 15 Å was used, to account for the effects due to other, mostly polar, residues of the protein surface. It was found that the susceptibility calculated for the protein interior assumes values in the range 12–15, and the susceptibility for the bulk water assumes a value of about 50. These values are in reasonable agreement with previous calculations on proteins[46] and neat water.[47]

The dielectric susceptibility in the membrane–protein interface depends on the distance between protein and membrane as well as on the region of the interface. For a sampling radius of 15 Å, the susceptibility of the membrane–protein interface shows maximum values between 40 and 50 for both simulation$^T$ and simulation$^L$. For a sampling radius of 10 Å, the dielectric susceptibility obtained from simulation$^L$ is approximately the same; however, a decrease in the susceptibility in the membrane head group region is observed for simulation$^T$, the maximum susceptibility at the membrane–protein interface being reduced to about 30. This result suggests that the hydrophobic residues of the enzyme IRS (Leu-2, Val-3, Ala-18, Leu-19, Phe-24, Val-31, and Phe-70) cause a slight dehydration in the membrane head group region in the tightly bound $PLA_2$–membrane complex and that such an effect is not detectable in the loosely bound $PLA_2$–membrane complex.

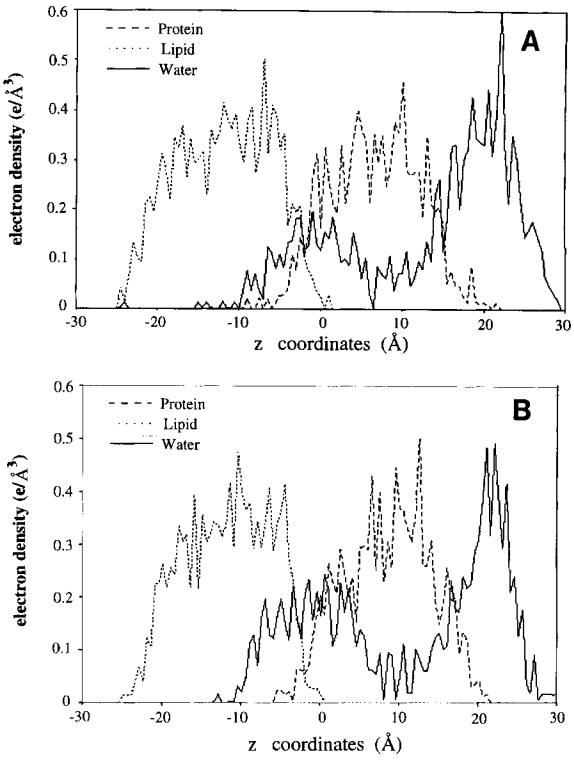


Fig. 4. Electron density profiles due to protein, lipid, and water molecules at 120 ps of simulation$^T$ (**A**) and simulation$^L$ (**B**) calculated for atoms within a radius of 15 Å from the $z$-axis.

## Energetic Properties

The interaction energies of the protein (including calcium ions) with itself and with the water molecules were calculated for simulation$^T$, simulation$^L$, and simulation$^A$, and are provided in Table I. The protein shows the lowest interaction energies with water and with itself in simulation$^A$. The losses in the protein–protein and protein–water interactions were compensated for by the protein–lipid interaction energies for simulation$^T$ and simulation$^L$.

To analyze the energetic properties of the lipid molecules in the $PLA_2$–membrane complexes, the lipid molecules were placed into two classes, class I if the distance of their second glycerol carbon atom to the $z$-axis lies within 25 Å, class II if the corresponding distance is between 25 and 35 Å. Lipid

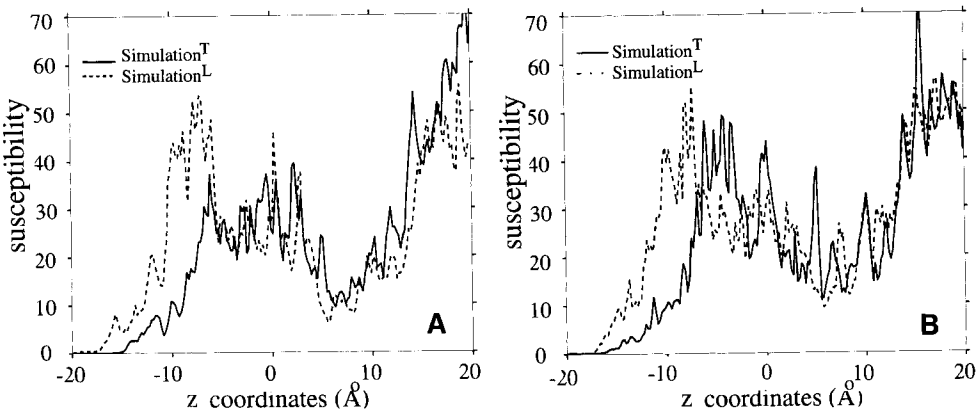


Fig. 5. Dielectric susceptibility along the *z*-axis in the protein-membrane interface calculated from simulation$^T$ and simulation$^L$. **A:** Atoms within a radius of 10.0 Å around the *z*-axis are included. **B:** Atoms within a radius of 15.0 Å around the *z*-axis are included.

**TABLE I. Average Protein-Protein, Protein-Water, and Protein-Lipid (all lipids in class I and class II) Interaction Energies**

| | Energy (kcal/mol) | | |
|---|---|---|---|
| Interaction | Simulation$^T$ | Simulation$^L$ | Simulation$^A$ |
| Protein-protein | −2,745.6 | −2,846.9 | −3,003.2 |
| Protein-water | −6,559.1 | −6,833.7 | −7,231.0 |
| Protein-lipid | −995.0 | −371.7 | — |

**TABLE II. Average Interaction Energies of the Lipid Molecules in Class I and Class II (see text; average values per lipid)**

| | Energy (kcal/mol) per lipid | |
|---|---|---|
| Interaction | Simulation$^T$ | Simulation$^L$ |
| Lipid(I)-protein | −18.05 | −7.73 |
| Lipid(II)-protein | −7.00 | −2.35 |
| Lipid(I)-lipid(I) | −187.80 | −191.20 |
| Lipid(II)-lipid(II) | −178.15 | −176.54 |
| Lipid(I)-water | −80.24 | −86.52 |
| Lipid(II)-water | −119.59 | −121.10 |

molecules in class I are located much closer to the enzyme, and some of the lipids actually form close contacts with it. The lipids in class II, however, are distant from the protein, and the properties of these lipids match those of lipids in a pure membrane–water system. The interaction energies were calculated for these two classes and are given in Table 2. Compared with the lipids in class II, the lipids in class I show a weaker interaction with the water molecules and stronger lipid–lipid interaction. The difference of the energetic properties of lipids in class I and class II is more drastic in simulation$^T$ than in simulation$^L$.

## Protein Structure

In general, the structure of PLA$_2$ remains highly stable during the molecular dynamics (MD) simulations. This is not surprising considering that PLA$_2$ has seven disulfide bonds and that homologous PLA$_2$s obtained from different species all have essentially the same structure, particularly around the active site.

The average root mean square (rms) deviation ($C_\alpha$ atoms only) of the MD average structure from simulation$^T$, simulation$^L$, simulation$^A$, and the structures reported in Scott et al.[14] and in Wery et al.[13] measure 1.50, 1.20, 1.23, and 1.26 Å, respectively. There are three regions that show large deviations, the deviations being observed not only for the MD structures, but also for the structure in Wery et al.[13] compared with the structure in Scott et al.[14] One can conclude, therefore, that the deviations reflect intrinsic flexibilities of the protein and are not an artifact of the simulation. In Figure 6, the averaged structures obtained from simulation$^T$, simulation$^L$, and simulation$^A$ and the two crystal structures are compared. Three regions that exhibit large fluctuations are indicated in Figure 6. The conformations of the protein active site in simulation$^T$, simulation$^L$, and simulation$^A$ are similar and are essentially identical to the X-ray structures (not shown).

## Ligation of Calcium Ions

The calcium ions bound in PLA$_2$ are ligated by protein groups and water molecules in simulation$^T$, simulation$^L$, and simulation$^A$. The force field used in the simulations does not employ geometric constraints for groups ligating with the calcium ion. As a result, the coordination geometry of the oxygen ligands observed in the X-ray crystal structure is not perfectly preserved. In simulation$^L$ and simulation$^A$ the two calcium ions are ligated by four protein ligands and four tightly associated water molecules (with the average distances between the

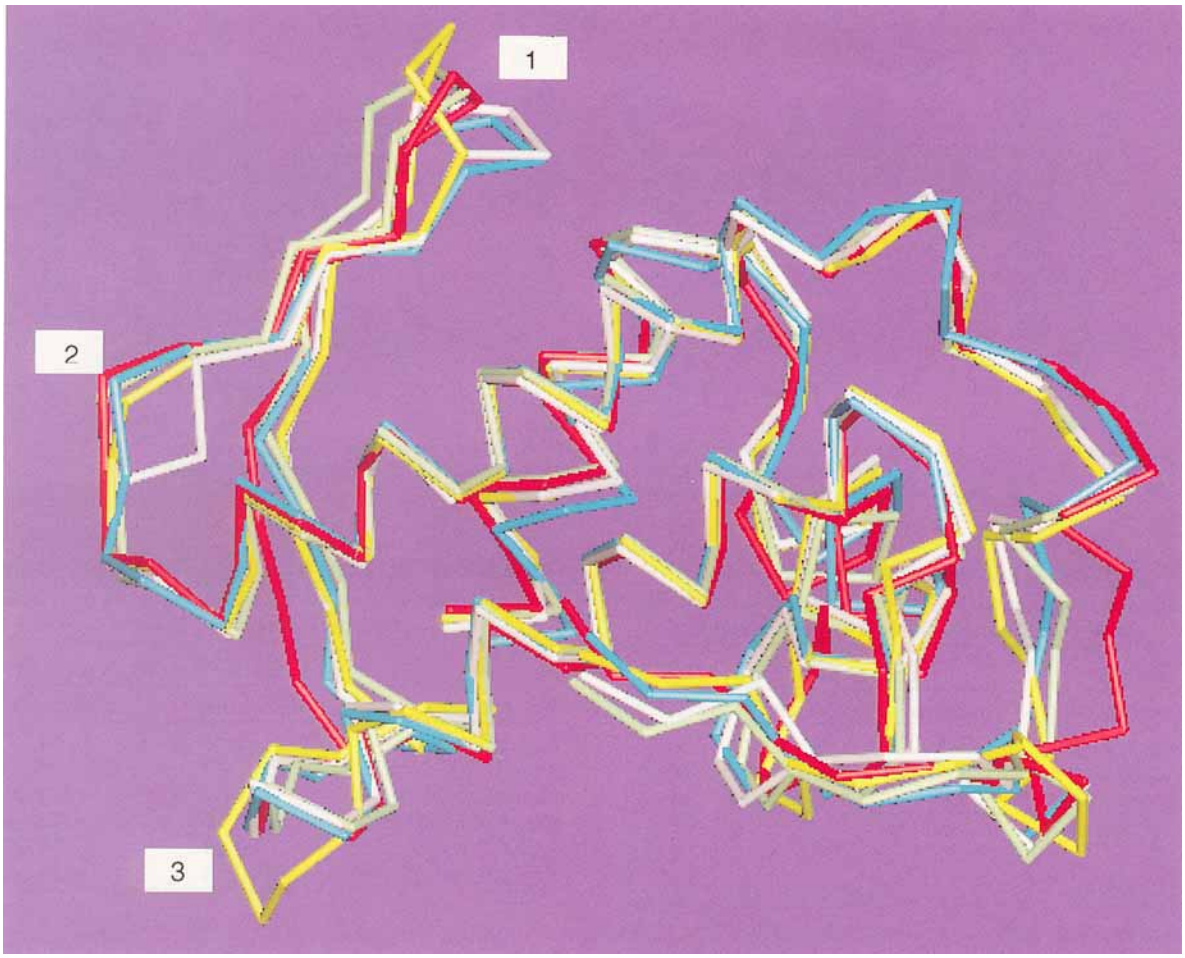


Fig. 6. Comparison of the averaged structure obtained from simulation$^T$, simulation$^L$ and simulation$^A$ with the crystal structures reported in Scott et al.[14] and Wery et al.[13]; only protein $C_\alpha$ atoms are presented. White, structure reported in Scott et al.[14]; yellow, structure reported in Wery et al.[13]; red, averaged MD structure from simulation$^T$, blue, averaged MD structure from simulation$^L$; green, averaged MD structure from simulation$^A$. The regions with large deviations between the structure are labeled as follows: region 1 includes residues Glu-55, Lys-56, Arg-57, and Gly-58; region 2 includes residues Gly-72 and Ser-73; and region 3 includes residues Lys-79 and Gln-80.

calcium and the water oxygen atoms less than 2.5 Å). In the structure obtained from simulation$^T$, however, the calcium ions interact with a lipid phosphate group either directly or via a water molecule. A total of seven ligands are observed for each of the two calcium ions. The number of water molecules associating with each calcium ion decreased during the simulation from 4 to 2–3. A large reduction in the number of waters ligating the calcium ion has also been suggested experimentally[29] for the $PLA_2$–substrate–membrane ternary complex. Our calculations suggest that such reduction might occur before the substrate is actually bound in the active site. A possible role of phosphate–calcium ligation for protein–membrane complexes has been suggested previously for calcium-containing proteins such as annexin.[48,49]

## Hydrogen Bonds and Salt Bridges Between Protein and Membrane

The simulations reveal that the penetration of protein residues into the membrane is not very deep, not even for complex$^T$. Only two residues, Phe-70 and Lys-23, penetrate the membrane to the glycerol backbone region. Charged residues such as Lys and Arg residues interact mostly with the lipid phosphate groups near the membrane surface. Residue Trp-3 in porcine pancreatic $PLA_2$, which has been well studied by fluorescence spectroscopy, is replaced by a much smaller sized Ile residue in the human synovial $PLA_2$, and it does not penetrate very far into the lipid head group region. The N-terminus of human synovial $PLA_2$ is found to be located in the surface of the lipid head group region in simulation$^T$.

The hydrogen bond interactions formed between the protein and lipid head groups have been analyzed for the structure at 120 ps of simulation$^T$. The criteria used in defining a hydrogen bond were the following: the distance hydrogen donor to hydrogen acceptor is less than 3.0 Å, and the angle between the donor-hydrogen-acceptor is less than 80°. Altogether 17 hydrogen bonds were found, including 7 between the lipid ethanolamine groups and the protein, 9 between lipid phosphate groups and the protein, and 1 between a lipid carbonyl group and the protein. Seven of these hydrogen bonds are salt bridges. The protein residues forming hydrogen bonds with the lipid molecules include Arg-7, Glu-16, Ala-18, Leu-19, Gly-23, Arg-34, Glu-56, Thr-68, Lys-69, Phe-70, Ser-72, Gln-118, Ser-121, Asn-122, Lys-123, and His-124. These groups are mostly located at the edge of the protein-membrane interface. The motion of the lipid head groups, on a picosecond time scale, is found to be moderately damped by hydrogen bonding interactions that arise through the binding of PLA$_2$ to the membrane surface; the rms fluctuations measure 40% less for lipids forming hydrogen bonds with the protein than for other lipids. On a longer time scale a decrease in lipid mobility has been observed[18] for negatively charged lipids interacting with PLA$_2$.

### Desolvation Effects of the Membrane Surface

The free energy changes of lipid head groups, when the charges of the $-CH_2NH_3^+$ and the $-CH_2PO_4^-CH_2$ groups were changed for simulation$^T_{reduced}$ from ±0.64 to ±1.0, were determined as described in Materials and Methods and are presented in Figure 7 mapped onto the membrane surface. Only a few lipid molecules located in the protein-membrane interface are found to be significantly desolvated. The desolvated lipids are all in contact with hydrophobic protein residues at the entrance to the binding site channel, whereas the majority of lipid molecules in the protein–membrane interface, interacting with polar or charged protein residues, show little difference in the solvation energy compared with that of bulk lipids.

The solvation free energy of the lipid head groups consists mainly of two contributions: a contribution due to charge–charge interaction, which depends linearly on the (positive and negative) charges $\pm q$ of the lipid head group, and a second contribution due to charge–induced dipole interaction, which depends quadratically on $q$. Accordingly, the free energy of the lipid head groups can be written

$$G_{solv}(q) = \alpha q + \beta q^2 \tag{2}$$

where $\alpha$ and $\beta$ are the coefficients weighting the two free energy contributions. The change of this energy upon recharging the lipids, i.e., adding charges $\pm\delta q$ to the head group is then

$$\frac{dG_{solv}}{dq}\delta q = (\alpha + 2\beta q)\delta q \tag{3}$$

i.e., depends linearly on the charge $q$. This quantity, save for the factor $\delta q$, is equivalent to the average electrostatic potential of the lipid head groups and can be evaluated from a molecular dynamics simulation; thereby the validity of Eq. 3 can be tested. For this purpose one determines for the moieties $-CH_2NH_3^+$ and $-CH_2PO_4^-CH_2^-$, defined as I and II in the following, for a given lipid labeled by the index $j$ the electrostatic energy with all partial atomic charges in the system. Let us define the respective energies $V_j(I;q)$ and $V_j(II;q)$. These energies, averaged over a molecular dynamics trajectory, are denoted as $\langle V_j(I;q)\rangle_s$ and $\langle V_j(II;q)\rangle_s$ where $s$ specifies the trajectory chosen, i.e., specified through the charges $\pm q$ assumed for the moieties $-CH_2NH_3^+$ and $-CH_2PO_4^-CH_2^-$. One finally averages the quantities over all 101 lipids, i.e., one evaluates

$$\overline{V_s(I;q)} = \frac{1}{101}\sum_{j=1}^{101}\langle V_j(I;q)\rangle_s. \tag{4}$$

The corresponding electrostatic potential for the complete head group, i.e., for both moiety I and II, is then

$$P_s(q) = \frac{1}{q}(\overline{V_s(I;q)} - \overline{V_s(II,q)}). \tag{5}$$

This quantity had been evaluated for simulation$^T_{reduced}$ assuming charge values $q = \pm 1.0$, $\pm 0.95$, $\pm 0.88$, $\pm 0.80$, and $\pm 0.70$ for moieties I and II. The resulting potential values showed a close to linear dependence on $q$. A linear regression fit of the computational results to Eq. 3 yielded $\alpha = 25.7$ kcal/(mol·e) and $\beta = -203.9$ kcal/(mol·e$^2$). The much larger magnitude of $\beta$ suggests that the solvation free energies of the phosphatidylethanolamine head groups are mainly determined by the charge–dipole interaction. This is expected since the lipid head groups are overall neutral in charge.

One can employ the estimate resulting from Eq. 5, i.e., the values for $\alpha$ and $\beta$ in Eq. 2, to determine the Coulomb contribution to the solvation energies of lipids. The energy, given by $G_{solv}(q = 1) = \alpha + \beta$ yields values between $-170$ and $-190$ kcal/mol. We are not aware of an experimental measurement of the solvation energy of the phosphatidylethanolamine head groups in the membrane, but one might compare the calculated value with the solvation free energies of $CH_3NH_3^+$[4] (experimental data)[50] and $PO_4^-$ (AM1-SM2 model prediction)[51] groups of $-75.0$ and $-105.5$ kcal/mol, respectively. The electrostatic potential energies of the lipid phosphate head groups in a membrane have also been previously calculated to be $-83.49$ kcal/mol by molecular dynamics simulation.[52]

The free energy difference experienced by lipids upon recharging from $q = \pm 0.64$ to $q = \pm 1.0$ shown in Figure 7 can serve as an estimate of the solvation energy difference between lipids in contact with hydrophobic groups of the enzyme (desolvated lipids) and of bulk lipids. From the data in Figure 7, evaluated according to Equation 1, we noticed that the energy difference measures about 4.5 kcal/mol between desolvated (blue in Fig. 7) and bulk (white in Fig. 7) lipids. This value corresponds to a $q = 0.64 \rightarrow q = 1$ recharging of the head groups. Linear extrapolation for a recharging $q = 0 \rightarrow q = 1$ yields a value of 7–8 kcal/mol. The value of 4.5 kcal/mol corresponds to the difference in the complete electrostatic solvation energy of the lipid head group. The value is small compared with the free energy difference of lipid molecules in a membrane bilayer and in solution (about 20 kcal/mol lower in membranes), but contributes a significant lowering of the energy barrier for insertion of the lipid head group in the active site. The desolvated lipids, which are interacting with hydrophobic protein residues located near the entrance of the enzyme active site, are ideally situated to induce an accelerated diffusion of lipids into the enzyme.

For simulation$^L$, we did not perform the free energy perturbation study by rescaling the charges. However, the difference in the free energies between $q = \pm 0.95$ and $q = \pm 1.0$ has been calculated for each lipid by means of the perturbation method from the trajectories obtained from simulation$^L$ ($q = \pm 1.0$) and compared with the corresponding energy for simulation$^T$. In the latter simulation, a few lipids (2–3) are observed to be significantly desolvated compared with the bulk lipids, a conclusion in agreement with the previous free energy calculations, but a significant desolvation of lipid head group was not found for simulation$^L$. This is consistent with the calculation of susceptibility profiles across the protein-membrane interface in which a decrease in the susceptibility of the membrane head group region is observed for simulation$^T$, but not for simulation$^L$ (Fig. 5).

## Charge-Charge Interactions Between Protein and Membrane

Free energy differences of the lipid head groups, when the charges of the lipid $CH_3NH_3^+$ groups ($q_+$) were changed from $+0.64$ to $+1.0$ (this alters the net charge on the lipid head group) were calculated using the perturbation method using trajectories obtained from simulation$^T_{negative}$. The results are shown in Figure 8, the free energy differences being mapped onto the membrane surface. The protein clearly favors binding of negatively charged lipids; however, this property is only observed for one part of the IRS, i.e., the positive electrostatic potential of the protein arises in a specific region, a feature that can be explained through the structural properties of the protein. The part of the protein surface that favors interaction with negatively charged lipids (the upper right side in Fig. 1) contains the two calcium ions (labeled in the figure) and a cluster of positive charged residues (colored in blue) at the protein C-terminal loop. Other parts of the protein, though also consisting of positively charged residues, do not show a strong preference for negatively charged lipids: these latter residues are either balanced by negatively charged residues (colored in red) or are located at positions that are accessible to bulk water; in contrast, the calcium ion II is buried in the protein-membrane interface, which does not shield charges as effectively.

The derivative of free energy changes of the lipid $CH_3NH_3^+$ groups $dG/dq_+$ can also be obtained through evaluation of the electrostatic potential of these groups in simulation$^T_{negative}$ and averaged over all lipid head groups as described above (see Eqs. 2–5). A linear relationship between $dG/dq_+$ and $q_+$ is observed (not shown), which further confirms that the free energy changes of the lipid head groups can be described by a charge–charge interaction term and a charge–induced dipole interaction term.

## Continuum Theory Calculations of the Electrostatic Potential at Protein-Membrane Interfaces

The electrostatic potential of $PLA_2$ was also determined in the framework of a continuum theory (Poisson-Boltzman equation) using the program GRASP.[53] The protein and lipid structure was taken from a snapshot of simulation$^T$ at 120 ps. The dielectric constant inside the protein and in the membrane was set to $\epsilon = 4.0$ and the dielectric constant in the solvent was set to $\epsilon = 78.0$; a 0.100 M salt concentration was assumed for all calculations.

The electrostatic potential was determined for the protein structure resulting from simulation complex$^T$. All charges of the protein and the lipid membrane have been included in the calculation, but water molecules were not included since a high

Fig. 7. Solvation free energy of lipid molecules mapped onto the membrane surface using the program GRASP.[53] The colors represent the free energy changes when charges of the ethanolamine and phosphate head groups were changed from $q = \pm 0.64$ to $q = 1.0$. Lipids with free energy changes of smaller magnitude, i.e., desolvated lipids, are shown in blue; lipids with larger free energy changes are shown in red; lipids with average free energy changes, i.e., bulk lipids, are shown in white. The protein is presented in green. Desolvation is observed for lipids interacting with protein hydrophobic residues; cf. Figure 1.

Fig. 8. Free energy changes of lipid molecules when the charges of the ethanolamine head groups are changed from $q_+ = 0.64$ to $q_+ = 1.0$. The free energy changes are mapped onto the membrane surface. Lipids with smaller free energy changes (negatively charged lipid favored compared with bulk lipids) are shown in blue; lipids with larger free energy changes (zwitterionic lipids favored compared with bulk lipids) are shown in red. The protein backbone is presented in green.

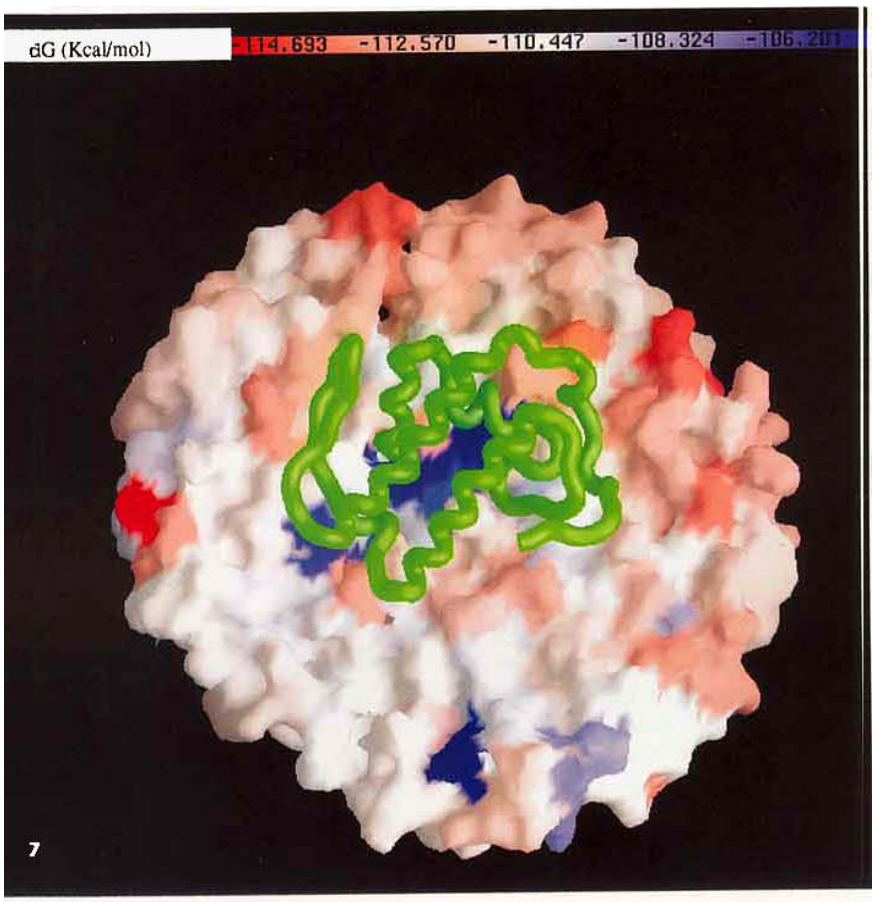
dG (Kcal/mol)
-114.693
-112.570
-110.447
-108.324
7

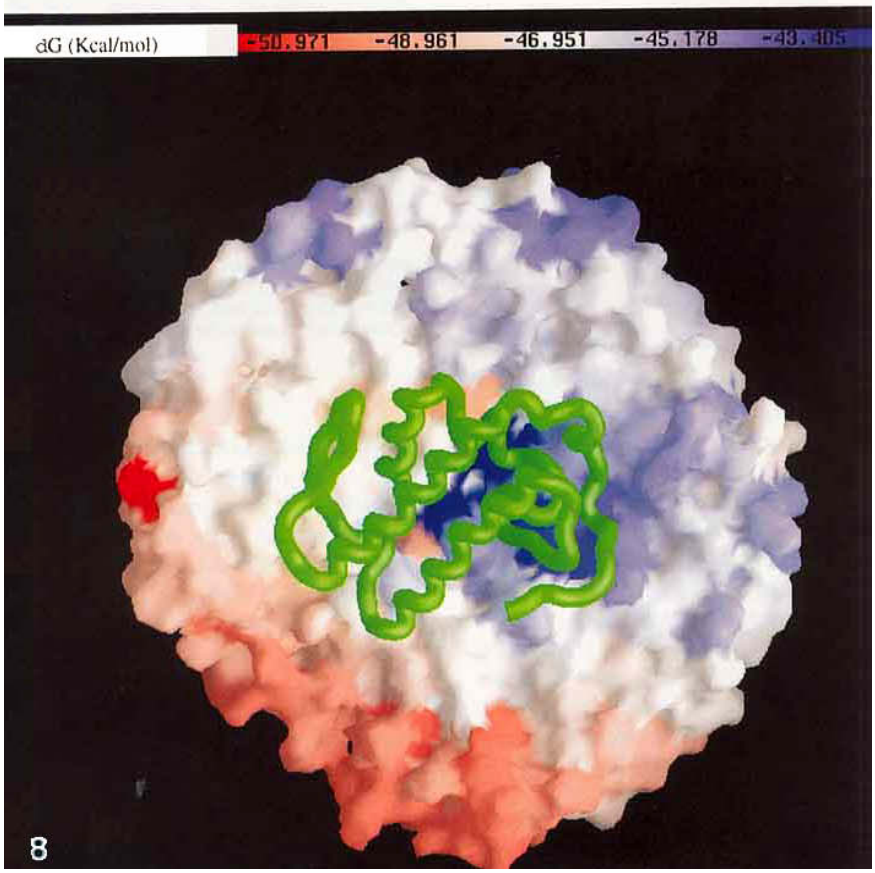
dG (Kcal/mol)
-50.971
-48.961
-46.951
-45.178
8

Figs. 7 and 8.

dielectric constant represents the solvent in the continuum description. Figure 9 shows that the electrostatic potential of the protein surface is predominantly positive for the protein–membrane complex. The potential energy is higher than that obtained for the protein without membrane using the structure of simulation$^A$ at 120 ps; this feature probably results from the low dielectric constant at the protein–membrane interface. The positive potential at the interface, however, decreased in a third calculation where the charges of the lipid $-CH_2NH_3^+$ groups were assumed to be +0.90 e and the total charge of each lipid was changed to −0.1 e. The resulting potential of the protein surface is also shown in Figure 9. An inhomogeneity of the protein surface potential is observed; the location of the protein surface with a highly positive electrostatic potential is in agreement with the free energy perturbation theory predictions described above.

The surface electrostatic potentials of ten $PLA_2$s from different species were determined in Scott et al.[54] It was observed that the potentials of $PLA_2$s show a clear sidedness, the IRS displaying a highly positive potential that depends sensitively on the number of calcium ions coordinated. Our calculations also indicate that calcium ions have a strong effect on the surface potential of human synovial $PLA_2$.

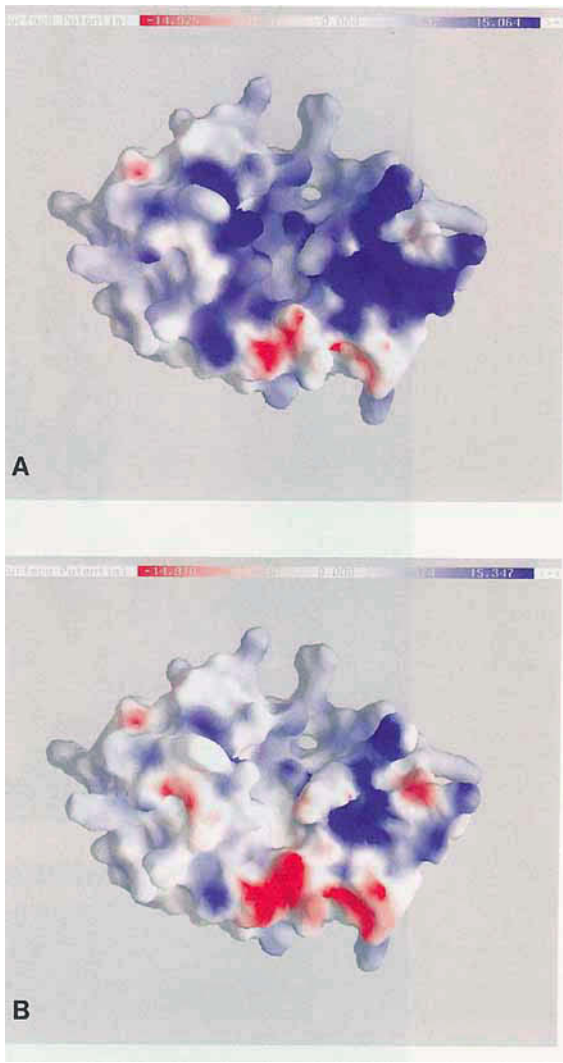


Fig. 9. Electrostatic potential on the $PLA_2$ surface for an enzyme-protein complex taken from simulation$^T$ at 120 ps. The potential shown is in units of $k_BT/e$. **A:** $PLA_2$ associated with a neutral membrane surface. **B:** $PLA_2$ associated with a negatively charged membrane surface, with a total charge per lipid of −0.1 e.

## DISCUSSION

Two phospholipase $A_2$-membrane complexes, a tightly bound complex$^T$ and a loosely bound complex$^L$, have been investigated in our study. The structure of the human synovial phospholipase $A_2$ was found not to change significantly on the membrane surface during the respective molecular dynamics simulations, a property expected from the known rigidity of the crystal structure.[8]

### Desolvation of Lipids at the Protein-Membrane Interface

A main emphasis of our study has been the energetics of the lipid head groups at the protein–membrane interface. Although lipid molecules are shielded from bulk water in the tightly bound protein–membrane complex, a change in the solvation free energy is observed for only a few lipid groups, namely, those that are interacting with the hydrophobic residues of the enzyme. Most of the lipid molecules in the protein–membrane interface, interacting with polar residues of the protein or interacting with the protein at the edge of the protein–membrane interface, do not show appreciable changes in the solvation free energy of their head groups.

It appears that the structure of the $PLA_2$ IRS, shown in Figure 1, is well suited to complex with the membrane surface and to enhance binding of the phospholipid substrate. The (mainly positively) charged residues of the protein, interacting with the lipid head groups in an environment with high dielectric constant, cannot be buried into the protein–membrane interface because the loss in solvation energies of a formal charge would be too large. Hydrophobic residues, however, do not interact strongly enough with the lipid head groups and probably are also not the best candidates to bind to the membrane surface. The polar residues in the protein–membrane interface, which can interact well with the mostly zwitterionic lipid head groups, can be buried in the interface at only moderate costs in Born energy due to the shorter range of dipole–dipole interactions compared with those of charge–dipole interactions. They are likely to be the best

choice to form a membrane-binding protein surface. Indeed, the major part of the $PLA_2$ IRS is formed by such residues, a situation similar to that found for the membrane-binding surface of annexin.[49]

Hydrophobic residues forming the entrance of the enzyme active site, however, play a key functional role. Dehydration of the lipid head groups by these residues should accelerate the diffusion of these lipids into the enzyme. To realize this function, only the hydrophobicity of the residues is important, i.e., the identity of these side groups does not need to be strictly conserved. Indeed, a wide variation of these residues among $PLA_2$s from different species is observed, but hydrophobicity is well conserved.[1] A collective mutation of these hydrophobic residues, which are shown in Figure 1, into polar ones, should affect the activation of the enzyme on the membrane surface, and thus might provide a test on the suggested effect of lipid desolvation to $PLA_2$ activity.

Desolvation of a few lipid head groups in the protein–membrane interface is observed, in this study, only for a tightly bound protein–membrane complex, as born out both by free energy calculations and by dielectric susceptibility calculations. No hints of such desolvation effect are found for a loose protein–membrane complex. The latter complex corresponds to a situation in which $PLA_2$ associates with membrane surfaces by long-range electrostatic attractions without penetrating with some of its residues into the membrane surface. The proenzyme of mammalian $PLA_2$s,[5,15] monoalogue modified $PLA_2$,[30] and $PLA_2$ bound on intact lecithin membranes probably form such loose complex.[55] Membrane defects, negatively charged lipid molecules, and other cofactors in the membrane might facilitate the penetration of a few protein residues into the membrane and cause the formation of fully functional, i.e., tight, $PLA_2$–membrane complexes.

The free energy calculations predict a solvation energy of $-170$ to $-190$ kcal/mol for the phosphatidylethanolamine head groups in the membrane, which compares favorably with known experimental and modeling data.[50,51] A 7–8 kcal/mol reduction in solvation energy is calculated for the lipid head groups interacting with the hydrophobic residues of the protein. The calculated free energy changes of the lipid head groups can be reasonably well approximated by a charge–charge interaction and a charge–dipole interaction, encouraging future macroscopic modeling studies of the lipid head groups in protein-membrane systems.

### Interaction Between $PLA_2$ and Negatively Charged Lipids

The charge–charge interactions between the protein and lipid molecules were studied using both free energy calculations and continuum theory electrostatic calculations. It was found that human synovial $PLA_2$ favors the binding of negatively charged lipid molecules, but the preference developed only from a fraction of the side groups of the IRS; calcium II and the protein C-terminus also seem to play an important role. The charge–charge interactions between the protein and the negatively charged membrane is likely to be stronger in the tightly bound protein–membrane complex, due to a lower dielectric constant in the local region and due to a closer distance between the protein and charged groups of the membranes. It would be interesting to see whether mutations of the protein residues that are involved in the ligation of calcium (II) or of residues at the C-terminus would affect the function of human synovial $PLA_2$ on negatively charged lipids.

### Limitations and Perspectives in Simulation Studies of $PLA_2$–Membrane Interactions

Our study demonstrates that molecular dynamics investigations of heterogeneous macromolecular systems are feasible today. The large size, the complexity of the system, and the long time scale required to study many physiologically relevant processes still make such investigations very challenging. However, using carefully designed computational procedures and a combination of modeling tools, some specific questions can be addressed.

Due to the pioneering nature of this study and limitations in available data, some assumptions presented here need to be further examined. For example, does the placement of a protein on the membrane surface in the two complexes studied reflect the true binding conformation of $PLA_2$ on a membrane? What are the factors that determine the penetration of $PLA_2$ into the membrane surface? Do molecular dynamics simulations equilibrate the water molecules in the protein–membrane interface sufficiently?

One important aspect of protein–membrane interactions that cannot be studied readily by molecular dynamics simulations at the present stage is the conformational changes of proteins on membrane surfaces. Recent NMR studies of phospholipase $A_2$ suggest that the N-terminus region of the protein is only ordered in the protein–inhibitor–micelle tertiary complex, causing formation of a hydrogen bonding network important for the enzyme catalysis.[45,34] Therefore, the difference in the activity of $PLA_2$ on a membrane surface and in solution could originate, at least partially, from the fact that $PLA_2$ in solution is not in a conformation optimal for the enzymatic reaction.

## ACKNOWLEDGMENTS

This study was initiated as a collaboration with Eli Lilly Research Laboratories. We thank Dr. Robert Bob Hermann, formerly at Eli Lilly, for numerous discussions and for providing us with structural data on human synovial phospholipase $A_2$. The research and the calculations for this paper were car-

ried out at the Resource for Concurrent Biological Computing funded by the National Institutes of Health (P41RRO5969). This work was also supported by the National Science Foundation (ASC93-18159) as well as by the Carver Charitable Trust.

## REFERENCES


1. Slotboom, A.J., Verheij, H.M., De Haas, G.H. On the mechanism of phospholipase $A_2$. In: "Phospholipids." Hawthorne, J.N., Ansell, G.B. (eds.). New York: Elsevier Biomedical Press, 1982:359–435.
2. Dennis, E.A. Phospholipases. In: "The Enzymes." Vol. XVI. New York: Academic Press, 1983:307–353.
3. Jain, M.K., Gelb, M.H., Rogers, J., Berg, O.G. Kinetic basis for interfacial catalysis by phospholipase $A_2$. Methods Enzymol. 249:567–614, 1995.
4. Vadas, P., Pruzanski, W. Role of secretory phospholipase $A_2$ in the pathobiology of disease. Lab. Invest. 55:391–398, 1986.
5. Verheij, H.M., Slotboom, A.J., de Haas, G.H. Structure and function of phospholipase $A_2$. Rev. Physiol. Biochem. Pharmacol. 91:91–203, 1981.
6. De Winter, J.M., Vianen, G.M., van den Bosch, H. Purification of rat liver mitochondrial phospholipase $A_2$. Biochim. Biophys. Acta 712:332–341, 1982.
7. Achari, A., Scott, D., Barlow, P., Vidal, J.C., Otwinowski, Z., Brunie, S., Sigler, P.B. Facing up to membranes: Structure/function relationships in phospholipases. Cold Spring Harbor Symp Quant Biol, Vol 52, 441–452, 1987.
8. Scott, D.L., White, S.P., Otwinowski, Z., Yuan, W., Gelb, M.H., Sigler, P.B. Interfacial catalysis: The mechanism of phospholipase $A_2$. Science 250:1541–1546, 1990.
9. Ramirez, F., Jain, M.K. Phospholipase $A_2$ at the bilayer interface. Proteins 9:229–239, 1991.
10. Dijkstra, B.W., Drenth, J., Kalk, K.H. The active site and the catalytic mechanism of phospholipase $A_2$. Nature 289: 604–606, 1981.
11. Dijkstra, B.W., Kalk, K.H., Hol, W.J.H., Drenth, J. Structure of porcine pancreatic phospholipase $A_2$ at 2.6 Å resolution and comparison with bovine phospholipase $A_2$. J. Mol. Biol. 147:97–123, 1983.
12. White, S.P., Scott, D.L., Otwinowski, Z., Gelb, M.H., Sigler, P.B. Crystal structure of cobra-venom phospholipase $A_2$ in a complex with a transition-state analogue. Science 250:1560–1563, 1990.
13. Wery, J.P., Schevitz, R.W., Clawson, D.K., Bobbitt, J.L., Dow, E.R., Gamboa, G., Goodson, Jr., T., Hermann, R.B., Kramer, R.M., McClure, D.B., Mihelich, E.D., Putnam, J.E., Sharp, J.D., Stark, D.H., Teater, C., Warrick, M.W., Jones, N.D. Structure of recombinant human rheumatoid arthritic synovial fluid phospholipase $A_2$ at 2.2 Å resolution. Nature 352:79–82, 1991.
14. Scott, D.L., White, S.P., Browning, J.L., Rosa, J.J., Gelb, M.H., Sigler, P.B. Structures of free and inhibited human secretory phospholipase $A_2$ from inflammatory exudate. Science 254:1007–1010, 1991.
15. Pierterson, W.A., Vidal, J.C., Volwerk, J.J., de Haas, G.H. Zymogen-catalyzed hydrolysis of monomeric substrates and the presence of a recognition site for lipid-water interfaces in phospholipase $A_2$. Biochemistry 13:1455–1460, 1974.
16. Jain, M.K., Yu, B.Z., Berg, O.G. Relationship of interfacial equilibria to interfacial activation of phospholipase $A_2$. Biochemistry 32:11319–11329, 1993.
17. Ghomashchi, F., Yu, B.-Z., Berg, O., Jain, M.K., Gelb, M.H. Interfacial catalysis by phospholipase $A_2$: Substrate specificity in vesicles. Biochemistry 30:7318–7329, 1991.
18. Volwerk, J.J., Post, P.C., de Haas, G.H., Griffith, O.H. Activation of porcine pancreatic phospholipase $A_2$ by the presence of negative charges at the lipid-water interface. Biochemistry 25:1726–1733, 1986.
19. Wilschut, J.C., Regts, J., Westenberg, H., Scherphof, G. Action of phospholipase $A_2$ on phosphatidylcholine bilayers. Effects of the phase transition, bilayer curvature and structural defects. Biochim. Biophys. Acta 508:185–196, 1978.
20. Burack, W.R., Yuan, Q., Biltonen, R.L. Role of lateral phase separation in the modulation of phospholipase $A_2$ activity. Biochemistry 32:583–589, 1993.
21. Op den Kamp, J.A.F., de Gier, J., van Deenen, L.L.M. Cobra venom phospholipase $A_2$: A review of its action toward lipid/water interfaces. Biochim. Biophys. Acta 345:253–256, 1974.
22. Verger, R., Mieras, M.C.E., de Haas, G.H. Action of phospholipase A at interfaces. J. Biol. Chem. 248:4023–4034, 1973.
23. Dennis, E.A., Darke, P.L., Deems, R.A., Kensil, C.R., Pluckthun, A. Cobra venom phospholipase $A_2$: A review of its action toward lipid/water interfaces. Mol. Cell. Biochem. 36:37–45, 1981.
24. Roberts, M.F., Deems, R.A., Dennis, E.A. Dual role of interfacial phospholipid in phospholipase $A_2$ catalysis. Proc. Natl. Acad. Sci. USA 74:1950–1954, 1977.
25. Brockerhoff, H. Substrate specificity of pancreatic lipase. Biochim. Biophys. Acta, 159:296–303, 1968.
26. Jain, M.K., Vaz, W.L.C. Dehydration of the lipid-protein microinterface on binding of phospholipase $A_2$ to lipid bilayers. Biochim. Biophys. Acta 905:1–8, 1987.
27. Jain, M.K., Maliwal, B.P. Spectroscopic properties of the states of pig pancreatic phospholipase $A_2$ at interfaces and their possible molecular origin. Biochemistry 32:11838–11846, 1993.
28. Mao, S.-Y., Maki, A.H., de Haas, G.H. Optically detected magnetic resonance studies of porcine pancreatic phospholipase $A_2$ binding to a negatively charged substrate analogue. Biochemistry 25:2781–2786, 1986.
29. van Scharrenburg, G.J.M., Slotboom, A.J., de Haas, G.H., Mulqueen, P., Breen, P.J., Horrocks, Jr., W.D. Catalytic $Ca^{2+}$ binding site of pancreatic phospholipase $A_2$: Laser-induced $Eu^{3+}$ luminescence study. Biochemistry 24:334–339, 1985.
30. Ghomashchi, F., Yu, B.-Z., Mihelich, E.D., Jain, M.K., Gelb, M.H. Kinetic characterization of phospholipase $A_2$ modified by monoalogue. Biochemistry 30:9559–9569, 1991.
31. Jain, M.K., Ranadive, G., Yu, B.-Z., Verheij, H.M. Interfacial catalysis by phospholipase $A_2$: Monomeric enzyme is fully catalytically active at the bilayer interface. Biochemistry 30:7330–7340, 1991.
32. Kramer, R.M., Pepinsky, R.B. Structure and properties of a human non-pancreatic phospholipase $A_2$. J. Biol. Chem. 264:5768–5775, 1989.
33. Pruzanski, W., Vadas, P. Secretory synovial fluid phospholipase $A_2$ and its role in the pathogenesis of inflammation in arthritis. J. Rheumatol. 15:1601–1603, 1988.
34. Parks, T.P., Lukas, S., Hoffman, A.F. Purification and characterization of a phospholipase $A_2$ from human osteoarthritic synovial fluid. In: "Phospholipase $A_2$." Wong, P.Y.K., Dennis, E.A. (eds.) New York: Plenum Press, 1990: 55–80.
35. Hara, S., Chang, H.W., Horigome, K., Kudo, I., Inoue, K. Purification of mammalian nonpancreatic extracellular phospholipase $A_2$. Methods Enzymol. Vol 211, 381–389, 1991.
36. Schevitz, R.W., Bach, N.J., Carlson, D.G., Chirgadze, N.Y., Clawson, D.K., Dillard, R.D., Draheim, S.E., Hartley, L.W., Jones, N.D., Mihelich, E.D., Olkowski, J.L., Snyder, D.W., Sommers, C., Wery, J.P. Structure-based design of the first potent and selective inhibitor of human non-pancreatic secretory phospholipase $A_2$. Nature Struct. Biol. 2:458–465, 1995.
37. Zhou, F., Schulten, K. Molecular dynamics study of a membrane-water interface. J. Phys. Chem. 99:2194–2208, 1995.
38. Alsina, A., Valls, O., Pieroni, G., Verger, R., García, S. Lipolysis by phospholipase $A_2$ of monomolecular mixed films of natural lipids. Colloid Polymer Sci 261:923–928, 1983.
39. Nelson, M., Humphrey, W., Gursoy, A., Dalke, A., Kalé, L., Skeel, R., Schulten, K., Kufrin, R. MDScope—a visual computing environment for structural biology. Comput. Phys. Commun. 91:111–134, 1995.
40. Humphrey, W.F., Dalke, A., Schulten, K. VMD—visual molecular dynamics. J. Mol. Graphics (in press).
41. Brünger, A.T. "X-PLOR, Version 3.1, A System for X-Ray Crystallography and NMR. The Howard Hughes Medical Institute and Department of Molecular Biophysics and

Biochemistry, Yale University. New Haven, CT: Yale University Press, 1992.
42. Brooks, B.R., Bruccoleri, R.E., Olafson, B.D., States, D.J., Swaminathan, S., Karplus, M. CHARMm: A program for macromolecular energy, minimization, and dynamics calculations. J. Comp. Chem. 4:187–217, 1983.
43. Windemuth, A. Advanced algorithms for molecular dynamics simulation: The program PMD. In: "Parallel Computing in Computational Chemistry." Mattson, T. (ed.). ACS Books, Washington, DC, 1995 (in press).
44. Zwanzig, R.W. High-temperature equation of state by a perturbation method. I. Nonpolar gases. J. Chem. Phys. 22:1420–1426, 1954.
45. van Gunsteren, W.F., Berendsen, H.J.C. Molekülдynamik-Computersimulationen; Methodik, Anwendungen und Perspektiven in der Chemie. Angew. Chemie 102:1020–1055, 1990.
46. King, G., Lee, F.S., Warshel, A. Microscopic simulations of macroscopic dielectric constants of proteins. J. Chem. Phys. 95:4366–4377, 1991.
47. Neumann, M. Dielectric relaxation in water. Computer simulations with the tip4p potential. J. Chem. Phys. 85: 1567–1576, 1986.
48. Creutz, C.E. The annexins and exocytosis. Science 258: 924–931, 1992.
49. Huber, R., Berendes, R., Burger, A. Crystal and molecular structure of human annexin V after refinement. Implications for structure, membrane binding and ion channel formation of the annexin family of proteins. J. Mol. Biol. 223:683–704, 1992.
50. Bartmess, J.E., McIver Jr, R.T. The gas-phase acidity scale. In: "Gas Phase Ion Chemistry," Vol. 2. Browers, M.T. (ed). New York: Academic Press, 1989:87–112.
51. Cramer, C.J., Truhlar, D.G. AM1-SM2 and PM3-SM3 parameterized SCF solvation models for free energies in aqueous solution. J. Comput. Aid. Mol. Des. 6:629–666, 1992.
52. Alper, H.E., Bassolino, D., Stouch, T.R. The limiting behavior of water hydrating a phospholipid monolayer: A computer simulation study. J. Chem. Soc. 99:5547, 1993.
53. Nicholls, A., Sharp, K.A., Honig, B. Protein folding and association: Insights from the interfacial and thermodynamic properties of hydrocarbons. Proteins 11:282–290, 1991.
54. Scott, D.L., Mandel, A.M., Honig, B. The electrostatic basis for the interfacial binding of secretory phospholipases $A_2$. Biophys. J. 67:493–504, 1994.
55. De Hass, G.H., Postema, N.M., Nieuwenhuizen, W., Van Deenan, L.L.M. Purification and properties of an anionic zymogen of phospholipase A from porcine pancreas. Biochim. Biophys. Acta, 159:103–117, 1968.
56. Peters, A.R., Dekker, N., van den Berg, L., Boelens, R., Kaptein, R., Slotboom, A.J., de Haas, G.H. Conformational changes in phospholipase $A_2$ upon binding to micellar interfaces in the absence and presence of competitive inhibitors. A $^1H$ and $^{15}NMR$ study. Biochemistry 31:10024–10030, 1992.
57. van den Berg, B., Tessari, M., Boelens, R., Dijkman, R., de Haas, G.H., Kaptein, R., Verheij, H.M. NMR structures of phospholipase $A_2$ reveal conformational changes during interfacial activation. Nature Struct. Biol. 2:402–406, 1995.